ChemPubSoc Europe
DOI: 10.1002/open.201600131
Open Access ChemistryOPEN Communications

The Blue–Violet Color of Pentamethylbismuth: A Visible Spin-Orbit Effect

Jeanet Conradie*[a] and Abhik Ghosh*[b]

Two-component relativistic time-dependent density functional theory calculations with spin-orbit coupling predict yellow and orange–red absorption for $BiPh_5$ and $BiMe_5$, respectively, providing an excellent explanation for their respective violet and blue–violet colors. According to the calculations, the visible absorption is clearly attributable to a single transition from a ligand-based HOMO to a low-energy LUMO with a significant contribution from a relativistically stabilized Bi 6s orbital. Surprisingly, scalar releativistic calculations completely fail to reproduce the observed visible absorption and place it at the violet/near-UV borderline instead.

Ever since their syntheses in the latter part of the 20th century, the violet color of pentaphenylbismuth[1,2] and the blue–violet color of pentamethylbismuth[3] have fascinated chemists.[4] For comparison, it might be noted that PPh_5, $AsPh_5$, and $SbPh_5$ are all colorless.[1,5,6] Surprisingly, despite the interest in the problem, the colors of $BiPh_5$ and $BiMe_5$ have not been investigated with modern quantum chemical methods. Early extended Hückel (EH)[7] calculations on BiH_5 and subsequent spin-orbit MS Xα[8] calculations on BiH_5 and $Bi(CCH)_5$ (CCH = ethynyl) correctly emphasized the key role of relativity on the lowest-energy electronic transition: "non-relativistic pentaphenylbismuth would not be violet." Importantly, the authors also noted a much lower transition energy for the C_{4v} square-pyramidal (SPy) form of BiH_5, relative to the D_{3h} trigonal-bipyramidal form. These early corrections did not deploy any specialized excited-state methodology and simply used a ΔSCF approach (the HOMO–LUMO gap) to predict transition energies. In the present reinvestigation of the problem, we studied $BiMe_5$, $BiPh_5$, and the as-yet unknown $Bi(CF_3)_5$ with modern ground-state density function theory (DFT) and time-dependent density functional theory (TDDFT) calculations based on the zeroth order regular approximation (ZORA)[9] to the two-component Dirac equation, applied with both spin-orbit coupling (SOC) and as a scalar correction.[10]

Scalar-relativistic OLYP[11] and/or B3LYP[12] geometry optimizations with large STO-TZ2P and QZ4P basis sets led to near-equienergetic TBP and SPy minima, with the latter less than 0.1 eV higher in energy than the former for all three molecules. In the case of $BiMe_5$, the transition state for the Berry pseudorotation connecting the two conformations was also located and found to be <1 kcal mol^{-1} higher in energy, relative to either conformer. The calculations thus appear to indicate a fluxional structure in solution for all three molecules.

These results are consistent with experimental studies on pentaarylbismuth derivatives, where the existence of both conformers in solution could be deduced from optical spectra; interestingly, their relative proportions were found to be independent of temperature, indicating near-identical thermodynamic stabilities.[7] Also, although the majority of pentaarylbismuth derivatives have exhibited SPy X-ray structures,[4] both $BiMe_5$[3] and a substituted pentaarylbismuth derivative have been found to exhibit TBP geometries.[7]

For both conformers of all three compounds studied, regardless of the functional, basis set, and relativistic treatment, our calculations indicate simple HOMO→LUMO character for the lowest-energy electronic transition (Figure 1 and Table 1).

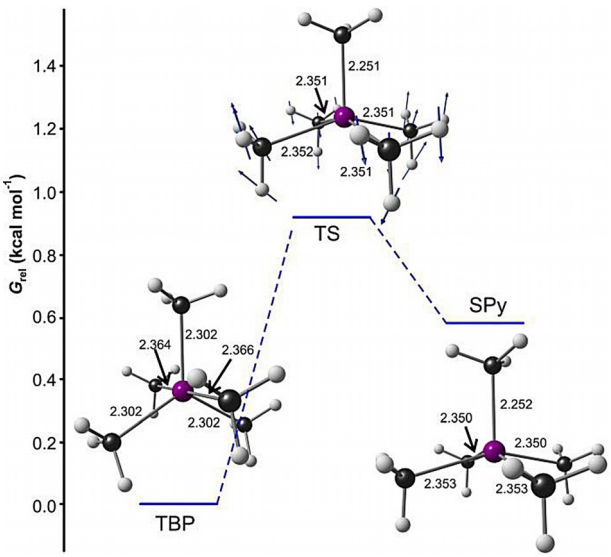

Figure 1. Gibbs free energies and geometries for the TBP, TS and SPy geometries of $BiMe_5$. $\Delta G^{\ddagger} = 0.92$ kcal mol^{-1} (0.040 eV), $\nu_i = 51.0i$ cm^{-1}.

[a] Prof. Dr. J. Conradie
Department of Chemistry
University of the Free State
9300 Bloemfontein (Republic of South Africa)
E-mail: conradj@ufs.ac.za

[b] Prof. Dr. A. Ghosh
Department of Chemistry
UiT–The Arctic University of Norway
9037 Tromsø (Norway)
E-mail: abhik.ghosh@uit.no

Supporting Information and the ORCID identification number(s) for the author(s) of this article can be found under http://dx.doi.org/10.1002/open.201600131.

© 2016 The Authors. Published by Wiley-VCH Verlag GmbH & Co. KGaA. This is an open access article under the terms of the Creative Commons Attribution-NonCommercial License, which permits use, distribution and reproduction in any medium, provided the original work is properly cited and is not used for commercial purposes.

© 2017 The Authors. Published by Wiley-VCH Verlag GmbH & Co. KGaA, Weinheim

Table 1. ZORA TDDFT results for the lowest-energy electronic transitions for $BiMe_5$, $BiPh_5$, and $Bi(CF_3)_5$.

Complex	Geometry	Functional	Relativistic approximation	Basis set	Excitation *l* [nm]	*E* [eV]	*f*	symmetry	% HOMO→LUMO
$BiMe_5$	TBP (C_{3v})	OLYP	scalar	TZ2P	382.6	3.24	1.39×10^{-14}	A_1	87.5
$BiMe_5$	TBP (C_{3v})	OLYP	spin-orbit	TZ2P	592.0	2.09	2.41×10^{-6}	E	99.6
$BiMe_5$	TBP (C_{3v})	OLYP	spin-orbit	QZ4P	617.2	2.01	3.18×10^{-6}	E	99.4
$BiMe_5$	TBP (C_{3v})	B3LYP	scalar	TZ2P	350.8	3.53	4.97×10^{-5}	A_1	97.4
$BiMe_5$	TBP (C_{3v})	B3LYP	spin-orbit	TZ2P	611.7	2.03	7.44×10^{-8}	E	97.9
$BiMe_5$	TBP (C_{3v})	B3LYP	spin-orbit	QZ4P	634.9	1.95	1.17×10^{-7}	E	97.1
$BiMe_5$	SPy (C_s)	OLYP	scalar	TZ2P	385.7	3.21	2.73×10^{-6}	A″	86.0
$BiMe_5$	SPy (C_s)	OLYP	spin-orbit	TZ2P	637.8	1.94	1.18×10^{-9}	A′	99.6
$BiMe_5$	SPy (C_s)	OLYP	spin-orbit	TZ2P	637.1	1.95	8.68×10^{-5}	A′	99.6
$BiMe_5$	SPy (C_s)	OLYP	spin-orbit	TZ2P	637.1	1.95	8.74×10^{-5}	A″	99.6
$BiMe_5$	SPy (C_s)	OLYP	spin-orbit	QZ4P	666.4	1.86	1.67×10^{-9}	A′	99.4
$BiMe_5$	SPy (C_s)	OLYP	spin-orbit	QZ4P	665.6	1.86	9.37×10^{-5}	A′	99.4
$BiMe_5$	SPy (C_s)	OLYP	spin-orbit	QZ4P	665.6	1.86	9.39×10^{-5}	A″	99.4
$BiMe_5$	SPy (C_s)	B3LYP	scalar	TZ2P	356.8	3.47	3.57×10^{-6}	A″	97.0
$BiMe_5$	SPy (C_s)	B3LYP	spin-orbit	TZ2P	717.2	1.73	9.16×10^{-10}	A′	98.1
$BiMe_5$	SPy (C_s)	B3LYP	spin-orbit	TZ2P	714.1	1.74	7.69×10^{-5}	A′	98.2
$BiMe_5$	SPy (C_s)	B3LYP	spin-orbit	TZ2P	714.1	1.74	7.64×10^{-5}	A″	98.2
$BiMe_5$	SPy (C_s)	B3LYP	spin-orbit	QZ4P	727.0	1.71	8.07×10^{-10}	A′	97.2
$BiMe_5$	SPy (C_s)	B3LYP	spin-orbit	QZ4P	723.7	1.71	8.37×10^{-5}	A′	97.3
$BiMe_5$	SPy (C_s)	B3LYP	spin-orbit	QZ4P	723.7	1.71	8.36×10^{-5}	A″	97.3
$BiPh_5$	TBP (C_2)[a]	OLYP	scalar	TZ2P	391.7	3.17	3.03×10^{-5}	A	90.6
$BiPh_5$	TBP (C_2)[a]	OLYP	spin-orbit	TZ2P	586.3	2.11	6.84×10^{-9}	A	99.3
$BiPh_5$	TBP (C_2)[a]	OLYP	spin-orbit	TZ2P	586.3	2.11	4.50×10^{-8}	B	99.3
$BiPh_5$	TBP (C_2)[a]	OLYP	spin-orbit	TZ2P	585.9	2.12	1.46×10^{-6}	B	99.4
$Bi(CF_3)_5$	TBP (C_{3v})	OLYP	scalar	TZ2P	425.5	2.91	1.29×10^{-6}	A_1	97.0
$Bi(CF_3)_5$	TBP (C_{3v})	OLYP	spin-orbit	TZ2P	825.9	1.50	1.44×10^{-6}	E	99.7
$Bi(CF_3)_5$	SPy (C_s)	OLYP	scalar	TZ2P	439.3	2.82	7.13×10^{-5}	A″	96.9
$Bi(CF_3)_5$	SPy (C_s)	OLYP	spin-orbit	TZ2P	993.1	1.25	6.27×10^{-7}	A′	99.7
$Bi(CF_3)_5$	SPy (C_s)	OLYP	spin-orbit	TZ2P	989.9	1.25	5.57×10^{-5}	A′	99.7
$Bi(CF_3)_5$	SPy (C_s)	OLYP	spin-orbit	TZ2P	989.9	1.25	5.64×10^{-5}	A″	99.7

[a] A "true" SPy structure could not be optimized; attempts at obtaining such a structure led to local minima intermediate between TBP and SPy geometries.

Furthermore, in each case, the HOMO was found to be an essentially ligand-based MO and the LUMO was found to have substantial (ca. 20%) Bi 6s character. These findings are qualitatively consistent with the notion that the color of $BiMe_5$ and $BiPh_5$ results from a low-lying LUMO, whose low energy (in spite of the Bi–C antibonding interactions shown in Figure 2) owes significantly to the relativistic stabilization of the Bi 6s level.

Quantitatively, the TDDFT calculations afforded a key surprise in that the scalar approximation completely fails to predict an absorption in the higher-wavelength visible range that would account for the blue–violet or violet color of $BiMe_5$ and $BiPh_5$. The ZORA-SOC calculations largely correct the problem, redshifting the transition energy by >200 nm to the orange and yellow parts of the spectrum, respectively (Table 1). By comparison, the choice of OLYP versus B3LYP has a relatively modest effect on the transition energy of $BiMe_5$, as does an STO-QZ4P versus TZ2P basis set. Thus, B3LYP results in a redshift of approximately 20 nm relative to OLYP, as does QZ4P relative to TZ2P. For the as-yet unknown $Bi(CF_3)_5$, ZORA-SOC predicts a transition energy in the near-IR, redshifted by 400 nm or more relative to the scalar relativistic value.

In qualitative agreement with EH and Xα calculations,[7,8] the SPy geometry results in a significant redshift in the transition

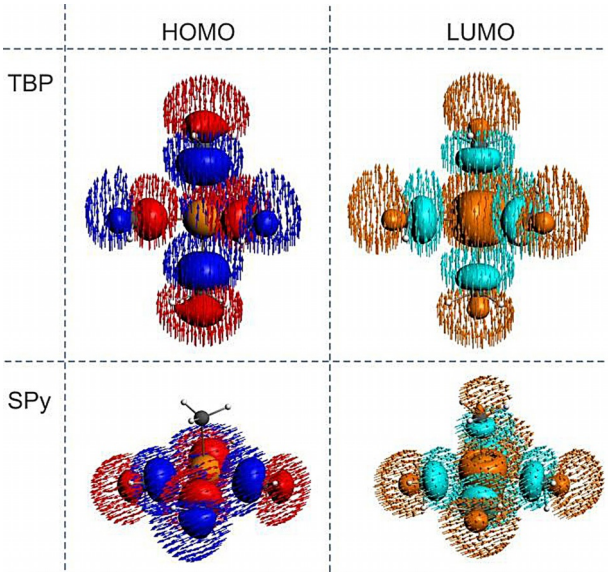

Figure 2. OLYP-ZORA-SOC/QZ4P spinor-MO overlays of the frontier orbitals for the two conformations of $BiMe_5$.

© 2017 The Authors. Published by Wiley-VCH Verlag GmbH & Co. KGaA, Weinheim

energy, relative to the TBP geometry. Depending on the exact methodological details, the redshift at the ZORA-SOC level is about 45–90 nm for $BiMe_5$ and 165 nm for the as-yet unknown $Bi(CF_3)_5$. Unlike $BiMe_5$ and $BiPh_5$, $Bi(CF_3)_5$ is thus predicted to be colorless.

In summary, two-component relativistic TDDFT calculations with spin-orbit coupling provide an excellent explanation for the blue–violet color of $BiMe_5$ and the violet color of $BiPh_5$. In contrast, scalar relativistic calculations are completely inadequate, overestimating the transition energies by 200 nm or more. The present results may be viewed as a cautionary tale that, although scalar relativistic calculations may afford a reasonable description of many aspects of sixth-row elements,[13,14] a correct description of spin-orbit effects may be essential for an accurate description of the electronic absorption spectra of 6p compounds.

Experimental Section

All DFT calculations were carried out with the ADF (Amsterdam Density Functional) 2014 program system,[15] employing the OLYP[10] GGA (generalized gradient approximation) or the B3LYP[11] hybrid functional, the ZORA[8] Hamiltonian applied with spin-orbit coupling or as a scalar correction, all-electron Slater-type TZ2P or QZ4P basis sets, a fine mesh for numerical integration, and full geometry optimizations with tight convergence criteria. Thermodynamic quantities were calculated as previously described[16] through the standard implementations in ADF. All TDDFT calculations with a given functional and basis set also employed molecular geometries optimized with the same functional and basis set.

Acknowledgements

This work was supported by FRINATEK grant 231086 of Research Council of Norway and by the National Research Fund of the Republic of South Africa. We gratefully acknowledge constructive comments from Professors Pekka Pyykkö and Konrad Seppelt on an earlier version of this paper.

Keywords: density functional calculations · pentamethylbismuth · pentaphenylbismuth · relativistic · spin-orbit effects

[1] G. Wittig, K. Clauss, *Justus Liebigs Ann. Chem.* **1952**, *578*, 136–146.
[2] A. Schmuck, J. Buschmann, J. Fuchs, K. Seppelt, *Angew. Chem. Int. Ed. Engl.* **1987**, *26*, 1180–1182; *Angew. Chem.* **1987**, *99*, 1206–1207.
[3] S. Wallenhauer, K. Seppelt, *Angew. Chem. Int. Ed. Engl.* **1994**, *33*, 976–978; *Angew. Chem.* **1994**, *106*, 1044–1046.
[4] B. Neumüller, K. Dehnicke, *Angew. Chem. Int. Ed. Engl.* **1994**, *33*, 1726–1728; *Angew. Chem.* **1994**, *106*, 1803–1805.
[5] a) P. J. Wheatley, C. Wittig, *Proc. Chem. Soc.* **1962**, 251–252; b) P. J. Wheatley, *J. Chem. Soc.* **1964**, 2206–2222.
[6] a) P. J. Wheatley, *J. Chem. Soc.* **1964**, 3718–3723; b) A. L. Beauchamp, M. J. Bennett, F. A. Cotton, *J. Am. Chem. Soc.* **1968**, *90*, 6675–6680.
[7] A. Schmuck, K. Seppelt, P. Pyykkö, *Angew. Chem. Int. Ed. Engl.* **1990**, *29*, 213–215; *Angew. Chem.* **1990**, *102*, 211–213.
[8] B. D. El-Issa, P. Pyykkö, H. M. Zanati, *Inorg. Chem.* **1991**, *30*, 2781–2787.
[9] a) E. van Lenthe, E. J. Baerends, J. G. Snijders, *J. Chem. Phys.* **1993**, *99*, 4597; b) E. van Lenthe, E. J. Baerends, J. G. Snijders, *J. Chem. Phys.* **1994**, *101*, 9783–9792; c) E. van Lenthe, A. Ehlers, E. J. Baerends, *J. Chem. Phys.* **1999**, *110*, 8943–8953.
[10] For a review on relativistic effects in chemistry, see: P. Pyykkö, *Annu. Rev. Phys. Chem.* **2012**, *63*, 45–64.
[11] a) The OPTX exchange functional: N. C. Handy, A. J. Cohen, *Mol. Phys.* **2001**, *99*, 403–412; b) The LYP correlation functional: C. Lee, W. Yang, R. G. Parr, *Phys. Rev. B* **1988**, *37*, 785–789.
[12] P. J. Stephens, F. J. Devlin, C. F. Chabalowski, M. J. Frisch, *J. Phys. Chem.* **1994**, *98*, 11623–11627.
[13] M. G. Goesten, C. Fonseca Guerra, F. Kapteijn, J. Gascon, F. M. Bickelhaupt, *Angew. Chem. Int. Ed.* **2015**, *54*, 12034–12038; *Angew. Chem.* **2015**, *127*, 12202–12206.
[14] R. F. Einrem, H. Braband, T. Fox, H. Vazquez-Lima, R. Alberto, A. Ghosh, *Chem. Eur. J. in press*, DOI: 10.1002/chem.201605015.
[15] The ADF program system uses methods described in: G. te Velde, F. M. Bickelhaupt, E. J. Baerends, C. F. Guerra, S. J. A. van Gisbergen, J. G. Snijders, T. Ziegler, *J. Comput. Chem.* **2001**, *22*, 931–967. For additional details, including the procedure for calculation of Gibbs free energies, see the ADF program manual: http://www.scm.com/ADF/.
[16] A. Ghosh, J. Conradie, *Eur. J. Inorg. Chem.* **2015**, 207–209.

Received: October 25, 2016
Published online on December 22, 2016

© 2017 The Authors. Published by Wiley-VCH Verlag GmbH & Co. KGaA, Weinheim